eJSE International

Electronic Journal of Structural Engineering (10) 2010

Performance of the PR connections under combined Axial-tension and moment loading

A. Pirmoz
Naghsh Afarin Mehraz Consulting Engineers, Iran
Email: a.pirmoz@gmail.com

M. M. Ahmadi & E. Valadi
University of Ilam, Iran
V. Farajkhah & S. R. Balanoji
Azar Parisab Consulting Engineers, Iran

ABSTRACT: The inherent moment capacity of bolted top-seat angle connections with double web angles (TSDW), categorized as partially restrained (PR) connections according to AISC-LRFD specifications, can be considered in analyses of semi-rigid connections especially when an accurate analysis of such fames is desired. However, in some cases, developed internal forces in the frame elements may affect the connection behavior, considerably. Axial tension force is one of such internal forces that may be imposed on frame connections in some cases such as construction imperfections, seismic loading or under large deflections of the catenary action during the progressive collapse of the semi-rigid frames. This study aims at the effects of the axial tension force on the performance of the bolted TSDW angle connections using nonlinear finite element method (FEM). The obtained results show that the axial tension force reduces the connection moment capacity and stiffness, considerably. Based on the obtained moment-rotation curves, affected by this particular loading type, equations are proposed to estimate the reduction rate of the connection stiffness and moment capacity.

1 INTRODUCTION

Bolted top-seat angle connections with double web angles (TSDW) - categorized as partially restrained (PR) connections according to AISC-LRFD specifications (AISC, 1995) - are widely used to support the vertical reaction of the steel beams. However, their considerable moment capacity makes it possible to take into account their contribution in the beam moment redistribution, deduction of the column's effective length (Kishi et al, 1997) and also the lateral resistance of the frame (Nader M N& Astaneh-Asl A, 1996; Danesh-Ashtiani F.A, 1996; Elnashai et al, 1998; Danesh F, 1999; Maison et al, 200; Akbas B, Shen J, 2003; Pirmoz A, 2006; Danesh F& Pirmoz A, 2007).

Lots of studies have done on the performance of bolted or riveted angle connections. Azizinamini (Azizinamini A, 1982; Azizinamini A, 1985) studied the effect of several geometrical properties of bolted TSDW on the connections moment-rotation characteristics. (Kukreti A R& Abolmaali A. S, 1999) studied the moment-rotation response of bolted top-seat angle under quasi-static loading and (Calado L, 2003) studied the cyclic response of the TSDW angle connections. Based on the obtained results, (Kukreti A R& Abolmaali A. S, 1999) proposed a few methods to estimate the moment-rotation behavior of bolted top & seat angles under cyclic loads. Pull test of bolted angles is a method to predict the moment-rotation response of bolted top and seat angle connections. (Garlock et al, 2003) and (Shen & Astaneh Asl, 1999; Shen & Astaneh Asl, 2000) studied the behavior of bolted angles under cyclic loads and proposed equations to predict the moment-rotation response of these types of connections.

Recently, FEM has become an efficient tool for studying the response of this type of connection. (Citipitioglu et al, 2002) performed a parametric study on the effects of the friction coefficient and the bolt pretension on the overall response of the bolted TSDW angle connections. (Pirmoz A, 2006) studied the applicability of the FEM in predicting the cyclic response of the bolted angle connections. He concluded the method is highly time-consuming despite its accuracy in predicting the connection response. (Danesh et al, 2007) studied the effects of the shear force on the initial stiffness of the bolted TSDW an-

gle connections and proposed an equation to estimate the reduction rate. (Pirmoz et al, 2008) showed that the web angle has a major role on the shear carrying capacity of these connections. Considering the shear strength of the web angles, they proposed an equation to estimate the reduction of the initial rotational stiffness of these connections. Their method showed a very good accuracy with respect to the method proposed by (Danesh et al, 2007). The effects of the axial tensional forces on the moment-rotation response of the bolted top-seat angle connections by Pirmoz et al (Pirmoz et al, 2009; Pirmoz et al, 2009). They proposed a method for predicting the moment-rotation response of this type of connection considering the reducing effects of the axial tensional forces. (Pirmoz A& Danesh F, 2009) showed that the seat angle has a considerable role on the moment-rotation response of the bolted top-seat angle connections, especially in the nonlinear range of the connection response. Performance of the bolted TSDW angle connections during progressive collapse of semi-rigid frames is studied by (Pirmoz A, 2009). The results showed that due to the arching action of the beam a considerable compressive force is applied on the connection that changes the response of the connection and the yielding mechanism and consequently the global performance of the frame can be affected. Based on the obtained results a method is proposed to estimate the affected response of the connection in progressive collapse condition. By sing artificial neural networks (ANN), (Pirmoz A& Gholizadeh S, 2007) and (Salajegheh et al, 2008) estimated the moment-rotation response of bolted angle connections, accurately.

None of the researches on the performance of the bolted TSDW angle connections relates to the behavior of this type of connection under combined axial tension and moment loading. Despite the fact that bolted TSDW angle connections are mainly designed to sustain the shear forces of the gravitational loads or to provide moment capacity for semi-rigid frames, in some cases, this type of connection may be subjected to large axial forces. Results of shaking table tests of (Nader M N& Astaneh-Asl A, 1996) revealed that during an earthquake, some axial forces may be imposed on connections. Due to the column removal in semi-rigid frames, after linear and arching stage (Pirmoz A, 2009), frame connections enter in catenary action phase and subject to a combined moment (of gravitational loads) and an increasing axial-tension force of the catenary action. Current study aims at the behavior of bolted TSDW angle connections under initial constant axial tension force and moment.

2 FE MODELING OF THE CONNECTION

2.1 *Characteristics of the connections*

The speciemens tested by Azizinamini (1982) consisted of two beams which were symmetrically connected to a stub column through bolted top and seat with double web angles (figure 1). The speciemens were in two groups which were different in the beam section, the stub column section and the number of the bolt rows of the web angles. The first group, named as 14SX scpesimens and the second group, 8SX, included relatively lighter specimens with two rows of the web angle bolts, shorter web angles and a W8×21 beam section. The clear distance between the beam and column flange was reported to be 12mm and the gap between the bolt shank and the hole was considered to be 1.6mm. Table (1) presents the geometry of the specimens. The bolts were high strength A325 bolts and the material of the angles, beams and stub columns was A36 steel.

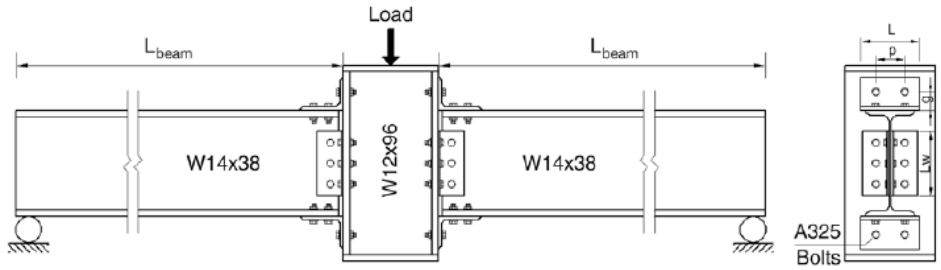

Figure 1. The test configuration

Table 1. Geometry of the connections

Specimen	Bolt diameter (mm)	Column section	Beam section	Top and Seat angle				web angle	
				angle	Length (mm)	Gauge(g) (mm)	Bolt spacing (p)(mm)	angle	Length (mm)
14S1	19.1	W12X96	W14X38	L6X4X3/8	20.32	63.5	13.97	2L4X3-1/2X1/4	215.9
14S2	19.1	W12X96	W14X38	L6X4X1/2	20.32	63.5	13.97	2L4X3-1/2X1/4	215.9
14S3	19.1	W12X96	W14X38	L6X4X3/8	20.32	63.5	13.97	2L4X3-1/2X1/4	139.7
14S4	19.1	W12X96	W14X38	L6X4X3/8	20.32	63.5	13.97	2L4X3-1/2X3/8	215.9
14S5	22.3	W12X96	W14X38	L6X4X3/8	20.32	63.5	13.97	2L4X3-1/2X1/4	215.9
14S6	22.3	W12X96	W14X38	L6X4X1/2	20.32	63.5	13.97	2L4X3-1/2X1/4	215.9
14S8	22.3	W12X96	W14X38	L6X4X5/8	20.32	63.5	13.97	2L4X3-1/2X1/4	215.9
8S1	19.1	W12X58	W8X21	L6X3-1/2X5/16	15.24	50.8	8.89	2L4X3-1/2X1/4	139.7
8S2	19.1	W12X58	W8X21	L6X3-1/2X3/8	15.24	50.8	8.89	2L4X3-1/2X1/4	139.7
8S3	19.1	W12X58	W8X21	L6X3-1/2X5/16	20.32	50.8	8.89	2L4X3-1/2X1/4	139.7
8S4	19.1	W12X58	W8X21	L6X6X3/8	15.24	137.2	8.89	2L4X3-1/2X1/4	139.7
8S5	19.1	W12X58	W8X21	L6X4X3/8	20.32	63.5	8.89	2L4X3-1/2X1/4	139.7
8S6	19.1	W12X58	W8X21	L6X4X5/16	15.24	63.5	8.89	2L4X3-1/2X1/4	139.7
8S7	19.1	W12X58	W8X21	L6X4X3/8	15.24	63.5	8.89	2L4X3-1/2X1/4	139.7
8S8	22.3	W12X58	W8X21	L6X3-1/2X5/16	15.24	50.8	8.89	2L4X3-1/2X1/4	139.7
8S9	22.3	W12X58	W8X21	L6X3-1/2X3/16	15.24	50.8	8.89	2L4X3-1/2X1/4	139.7
8S10	22.3	W12X58	W8X21	L6X3-1/2X1/2	15.24	50.8	8.89	2L4X3-1/2X1/4	139.7

2.2 *FE modeling of the connections*

The modeling is done by ANSYS multy-purpose finite element modeling code. Implementing ANSYS Parametric Design Language (APDL), parametric FE models are created while the geometrical and mechanical properties of the connections were as the parameters.

Numerical modeling of the connection is done including following considerations: all components of connection such as beam, column, angles and bolts are modeled using eight node first order SOLID45 elements and bolt shanks are modeled using SOLID64 element which can consider thermal gradient used to apply pretensioning force on bolts. Only half of the connection is modeled because of the symmetry exists about the web plane. Since the stub column and the beams were strong enough with respect to the connections, these segments remained elastic and thus negligible deformations were expected to occure in the beam, column flanges and web. The interaction between adjacent surfaces, including angle-beam flange, bolt head-nut, bolt hole-bolt shank and also the effect of friction were modeled using CONTA174 and TARGE170 contact elements. This proper modeling of the component interactions acquires the interaction between the nut and the head with the corresponding surfaces when a negative thermal gradient is applied on the bolt shank and this restraining, pretensions the bolts. 178 kN pretensioning force is applied to 22.3 mm bolt diameter and 133 kN for 19.1 mm bolt diameter. Figure (2-a) presents the FE model of the 14S2 specimen and figure (2-b) shows its deformed shape.

More information about the modeling, material properties and validating the FE models are presented in (Pirmoz A, 2006; Danesh et al, 2007; Pir-

moz et al, 2008; Pirmoz et al, 2008; Pirmoz et al, 2009; Pirmoz A& Danesh F, 2009; Pirmoz A, 2009; Pirmoz A& Gholizadeh S, 2007; Salajegheh et al, 2008).

Moment-rotation responses of two models are presented in fig. (3). A relatively fair accuracy is obtained for FE models. A peer discussion on the accuracy of the models and the sources of the error are documented in the previous works by the frist author (Pirmoz A, 2006; Danesh et al, 2007; Pirmoz et al, 2008; Pirmoz et al, 2008; Pirmoz et al, 2009; Pirmoz A& Danesh F, 2009; Pirmoz A, 2009; Pirmoz A& Gholizadeh S, 2007; Salajegheh et al, 2008).

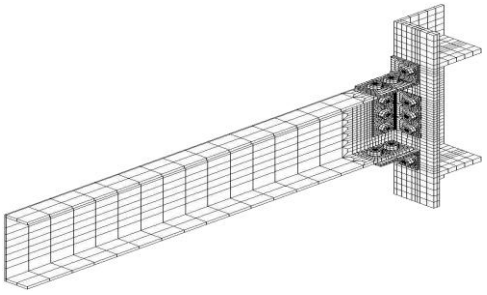

a. FE modeling of 14S2 by 16562 elements

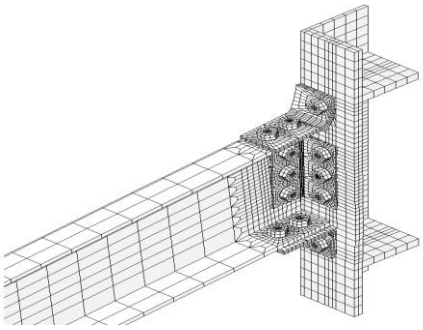

b. deformed shape of 14S2 at 0.03 rad, Scaled by 2

Figure 2. FE mesh pattern and deformed shape of the 14S2

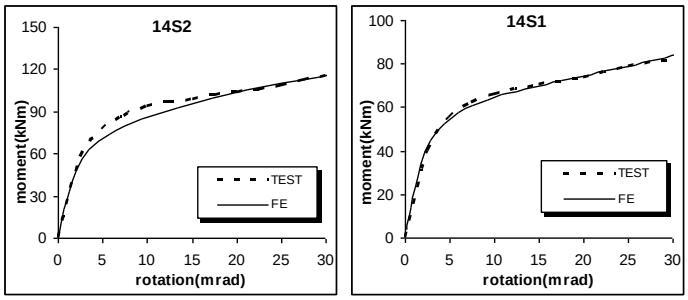

Figure 3. Comparison between the results of the FE and test

3 EFFECT OF AXIAL TENSION FORCE ON CONNECTION BEHAVIOR

As cited previously, variable or constant axial forces could be developed in the frames connections during an earthquake (Nader M N& Astaneh-Asl A, 1996), progressive collapse (Pirmoz A, 2009) or during the construction processes. Fig. (4) presents the axial tension-axial deflection curve of the 14S8 specimen at the beam end, where the axial load is imposed. As seen from this figure, after 1.0mm axial deflection, which corresponds to an almost 420 kN axial force, the beam slippage starts (the horizontal part of the curve). This horizontal portion of the curve almost equals to the gap distance between the bolt shank and the beam or the angle hole. After approximately 1.5 mm slippage, connection axial stiffness recovers due to the contact of the bolt shank and the surface of the hole. The curve includes the axial deformations of the beam which is ignoring because of the relatively higher axial stifnness of the beam.

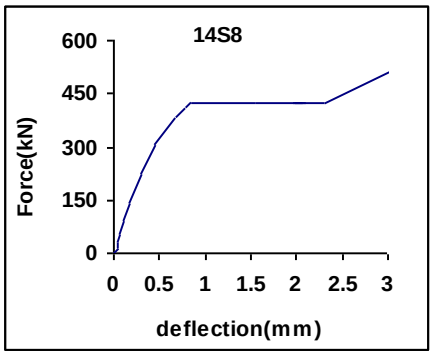

Figure 4. axial tension-axial deflection curve of the 14S8 connection

The effects of the axial tensional force on the moment-rotation response of the connections are studied in this section. For this purpose, after applying the bolts pretension, an axial tensional force is applied on the nodes of the beam end as the second load case and then the monotonic moment loading is applied on the connection by downward pushing of the beam end. The imposed load on the connection during the stated loading conditions can also be increasing (monotonic). However, the studies by (Pirmoz et al, 2009) showed that the constant axial tensional force has a sever effect on the connection. Ac-Accordingly, the current study considers only the constant axial loading which is combined with monotonic moment loading. Five specimens of Azizinamini's tests are selected randomly and each specimen is analyzed under five different magnitudes of the axial tensional force and monotonic moment loading. The name of the specimens and the magnitude of the applied axial-tensional forces on the con-

nections are listed in table (2). A total of 25 models under axial tension and moment loading are analyzed.

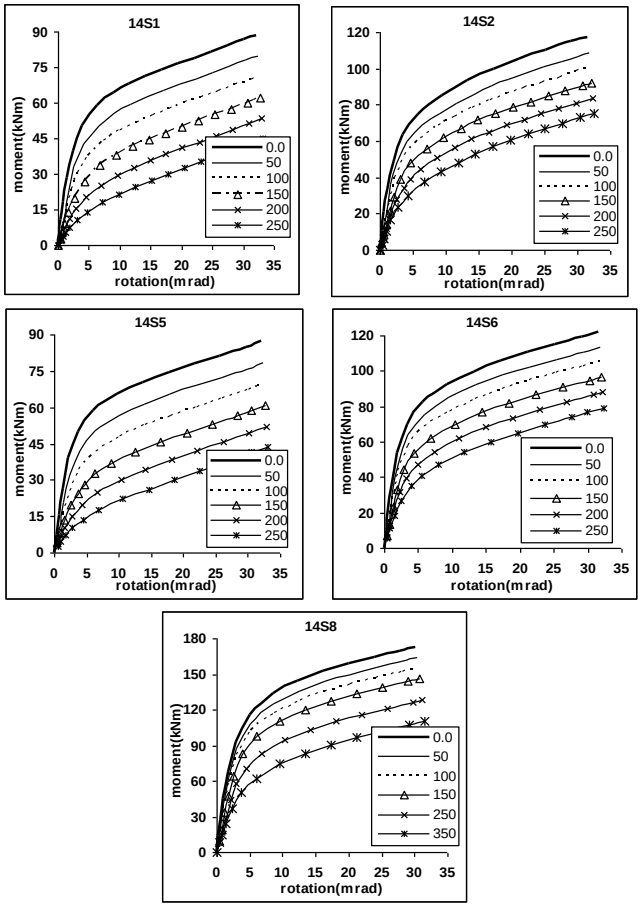

Figure 5. Moment-rotation response of the connections under combined tension (kN) and moment (kNm)

Moment-rotation response of the connections under different loading magnitudes is shown in figure (6). As seen from this figure, axial tensional load decreases the connection initial stiffness and its moment capacity. The numbers assigned for each curve denotes the magnitude of the applied axial force on the connection. Since the 14S8 has relatively higher moment capacity with respect to other four connections, greater axial load, 350 kN, is applied on it to observe a sensible reduction on its response.

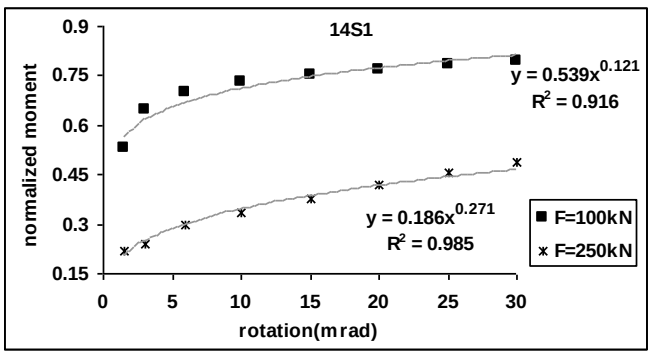

Figure 6. Plots of M_t/M_o for 14S1 specimen

4 DATA PROCESSING

To estimate the moment-rotation curve of the connection under combined axial tension and moment loading, the rate of the changes in the moment-rotation response of the connection due to the applied axial load is studied first. To achieve this, the ratio of Mt/Mo is plotted against the connection rotation for each specimen. In which, Mt is the reduced moment capacity of the connection due to the applied axial tension force and Mo denotes its moment capacity without any axial force at a given rotation. The plots of the Mt/Mo are shown in figure (6) for 14S1 specimen under 100 kN and 250 kN of axial force. It can be seen that the rate of the moment changes is almost linear for rotations larger than 0.005 radians. Within smaller rotations, moment capacity of the connection is more affected. Increasing of the connection rotation decreases the sensitivity of the connection response to the applied axial force. For each series of the data, a curve is fitted using interpolation technique. Table (2) presents the equations of the fitted curves for each model.

Table 2. Equations of the fitted lines for each FE model

Number	Specimen	Axial force (kN)	Equation of the fitted curve	R2
1	14S1	50	$0.758R^{0.053}$	0.90
2	14S1	100	$0.539R^{0.121}$	0.92
3	14S1	150	$0.42R^{0.148}$	0.96
4	14S1	200	$0.301R^{0.190}$	0.99
5	14S1	250	$0.186R^{0.271}$	0.99
6	14S2	50	$0.851R^{0.026}$	0.91
7	14S2	100	$0.690R^{0.066}$	0.85
8	14S2	150	$0.555R^{0.108}$	0.91
9	14S2	200	$0.449R^{0.136}$	0.99
10	14S2	250	$0.358R^{0.184}$	0.99
11	14S5	50	$0.760R^{0.051}$	0.92
12	14S5	100	$0.549R^{0.112}$	0.95
13	14S5	150	$0.422R^{0.141}$	0.99
14	14S5	200	$0.303R^{0.182}$	0.98
15	14S5	250	$0.183R^{0.269}$	0.97
16	14S6	50	$0.868R^{0.022}$	0.83
17	14S6	100	$0.722R^{0.055}$	0.88
18	14S6	150	$0.595R^{0.087}$	0.92
19	14S6	200	$0.492R^{0.1106}$	0.99
20	14S6	250	$0.399R^{0.136}$	0.99
21	14S8	50	$0.896R^{0.0176}$	0.91
22	14S8	100	$0.785R^{0.0416}$	0.90
23	14S8	150	$0.694R^{0.061}$	0.85
24	14S8	250	$0.535R^{0.098}$	0.95
25	14S8	350	$0.410R^{0.126}$	0.99

As seen from table (2), it is clear that an equation in its general form of eq. (1) can estimate the connection response under a specific axial tensional force, accurately.

$$y = ax^b \quad (1)$$

However, for engineering applications, a general equation is needed to estimate a given connection response, affected by a given axial load. Practical connections vary considerably in their geometrical and mechanical properties. On the other hand, the effects of such properties reflect on the connection moment-rotation response characteristics, such as its initial stiffness or moment capacity.

The yield moment is one of the major characteristics of the connection. Figure (7) illustrates the way for determining the *yield moment*, M_y. This parameter is used later as a representative of the connection moment-rotation response.

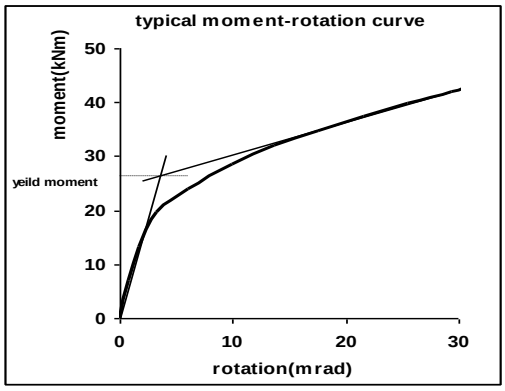

Figure 7. Visual illustration of the connection yield moment

Another parameter is defined for the connections as the *equivalent moment*, M_e. The effect of the axial tensional force on the connection angles is set to be equal with the effect of a corresponding moment loading. In other words, the horizontal displacement of the top angle due to a given tensional load needs a moment, M_e, which can be calculated using eq. (2). Visual illustration of the method is presented in figure (8).

$$M_e = Fh/4` \quad (2)$$

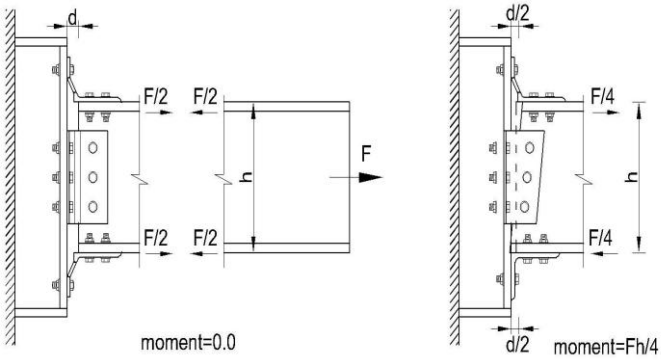

Figure 8. Visual illustration of the equivalent moment of tension force determination

Table (3) list the "a" and "b" of equation (1) for the equations presented in table (1). The "a" and "b" of each equation of table (2) are plotted against the ratio of M_e/M_y. Table (2) also contains the M_e and M_y properties of each model.

Table 3. Equivalent, yield moments and axial forces of models

specimen	force(kN)	Me(kN.m)	My(kN.m)	Myt/My	a	b
14S1	50	4.5	60	0.07	0.758	0.053
14S1	100	9.0	60	0.15	0.539	0.121
14S1	150	13.4	60	0.22	0.420	0.148
14S1	200	17.9	60	0.30	0.301	0.190
14S1	250	22.4	60	0.37	0.186	0.271
14S2	50	4.5	84.9	0.05	0.851	0.026
14S2	100	9.0	84.9	0.11	0.690	0.066
14S2	150	13.4	84.9	0.16	0.555	0.108
14S2	200	17.9	84.9	0.21	0.449	0.136
14S2	250	22.4	84.9	0.26	0.358	0.184
14S5	50	4.5	60.6	0.07	0.760	0.051
14S5	100	9.0	60.6	0.15	0.549	0.112
14S5	150	13.4	60.6	0.22	0.422	0.141
14S5	200	17.9	60.6	0.30	0.303	0.182
14S5	250	22.4	60.6	0.37	0.183	0.269
14S6	50	4.5	91.2	0.05	0.868	0.022
14S6	100	9.0	91.2	0.10	0.722	0.055
14S6	150	13.4	91.2	0.15	0.595	0.087
14S6	200	17.9	91.2	0.20	0.492	0.1106
14S6	250	22.4	91.2	0.25	0.399	0.136
14S8	50	4.5	135.9	0.03	0.896	0.0176
14S8	100	9.0	135.9	0.07	0.785	0.0416

14S8	150	13.4	135.9	0.10	0.694	0.061
14S8	250	22.4	135.9	0.16	0.535	0.098
14S8	350	31.3	135.9	0.23	0.410	0.126

Plots of "a" and "b" against the ratio of M_e/M_y, shown in figure (9), clarify that a second-order polynomial equation would be considered between these parameters and the ratio of M_e/M_y.

According to figure (9) and a little simplification "a" and "b" parameters could be calculated by eq. (3, 4):

$$a = 2.84\left(\frac{M_e}{M_y}\right)^2 - 3.21\left(\frac{M_e}{M_y}\right) + 1 \quad (3)$$

$$b = 0.55\left(\frac{M_e}{M_y}\right)^2 + 0.48\left(\frac{M_e}{M_y}\right) + 0.01 \quad (4)$$

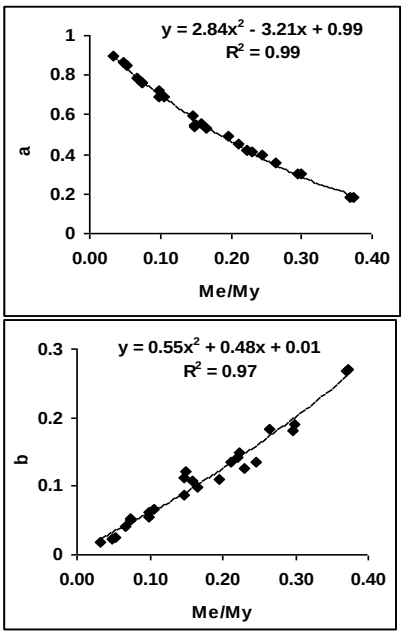

Figure 9. Plots of "*a*" and "*b*" parameters against M_e/M_y.

Replacing eq. (3) and (4) in eq. (1) and yields the affected moment values for a given rotation, R, and the applied axial-tension force, F in form of equation (5).

$$M_t = M_0.a.R^b \quad (5)$$

To examine the accuracy of the proposed equation for models beyond the studied models, two different connections, 14S3 and 8S1 specimens, are chosen and analyzed under 150 and 100 (kN) axial tension force, respectively. The response of the connections, obtained by FEM, agrees well with results of eq. (5). Figure (10) shows the comparisons between the results of FEM and eq. (5).

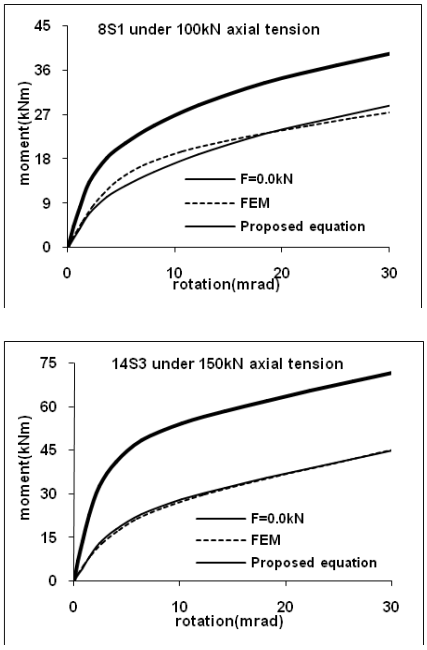

Figure 10. Comparisoning the results of FEM and eq. (7)

5 CONCLUSION

Axial tensional forces, developed in the connections of a semi-rigid frame during seismic excitations, construction tolerances or other probable causes, affect the connection moment-rotation response considerably. Using nonlinear FEM, a method is presented to estimate the moment-rotation response of bolted TSDW angle connections under combined axial tensional forces and monotonic moment loading. All the connection components are modeled using solid elements and the contact elements are used to take into account the effect of the interaction of the adjacent components of the connection. Applying a negative thermal gradient on the bolts shanks, the bolts pretension force is applied as the first load case. Several FE models of previously tested specimens are created and analyzed under combination of different magnitudes of the axial-tension and monotonic moment loading. Results of analyzing these models cleared that the axial-tension force decreases the connection initial rotational stiffness, moment capacity and energy absorbance capacity. Altering the applied axial tensional force into an equivalent

moment and dividing this value by the yield moment of the connection, a series of dimensionless data are obtained. Then, by using interpolation technique a formula is suggested to estimate the moment-rotation curve of the connection under combined tension-moment loading. Comparing the accuracy of the proposed equation with those obtained by FEM showed that the method has a good accuracy and can be used easily for engineering applications.

REFERENCES

[1] AISC, Manual of steel construction-Load and resistance factor design, American Institute of Steel Construction, Chicago, ILL, 1995
[2] Akbas B, Shen J. Seismic behavior of steel buildings with combined rigid and semi-rigid frames. Turkish J. Eng. Env. Sci. 2003; 27:253-264.
[3] Azizinamini A, Cyclic Characteristic of bolted semi-rigid steel beam to column connections, PhD thesis, University of South Carolina, Columbia, 1985.
[4] Azizinamini A, Monotonic response of semi-rigid steel beam to column connections, MS thesis, University of South Carolina, Columbia, 1982.
[5] Calado L. Non-linear cyclic model of top and seat with web angle for steel beam-to-column connections, Engineering Structures, 2003; 25:1189-1197
[6] Citipitioglu A.M., Haj-Ali R.M., White D.W. Refined 3D finite element modeling of partially restrained connections including slip. Journal of construct steel research, 2002; 8:995-1013.
[7] Danesh F, Pirmoz A. Numerical modeling of top and seat angle connections with double web angles, 9th Canadian conference on earthquake engineering. Ottawa, Ontario, Canada, June 2007, Paper No.1024.
[8] Danesh F., Nonlinear dynamic analyses of semi-rigid steel frames and comparison with test results. 3rd International conference of Seismology and Earthquake Engineering, May 1999, Tehran, Iran.
[9] Danesh F., Pirmoz A., Saedi Daryan A. Effect of shear force on the initial stiffness of top and seat angle connections with double web angles. Journal of Constructional Steel Research 2007; 63:1208-1218.
[10] Danesh-Ashtiani F. A. Seismic performance of steel frames with semi-rigid connections. PhD thesis, (London) England: Imperial Collage of Science, Thecnol and Medicine, Univ. of London; 1996.
[11] Elnashi A.S, Elghazouli A. Y, Danesh-Ashtiani F. A. Response of semi-rigid steel frames to cyclic and earthquake loads. Journal of structural Engineering 1998; 124(8):857-67.
[12] Garlock M., Ricles J. M., Sause R. Cyclic load tests and analysis of bolted top-and-seat angle connection. Journal of structural Engineering 2003; 129(12):1615-25.
[13] Kishi N., Chen W. F., Goto Y. Effective length factor of columns in semirigid and unbraced frames, Journal of structural Engineering, ASCE; 1997; 123(3); 0313-0320.
[14] Kukreti A R, Abolmaali A. S, Moment-Rotation hysteresis behavior of top and seat angle steel frame connections, Journal of structural Engineering, ASCE; 1999; 125(8); 0810-20.
[15] Maison B F, Rex C O, Lindsey S D, Kasai K. Performance of PR moment frame buildings in UBC seismic zones 3 and 4, Journal of Structural Engineering 2000;ASCE; 126(1), 0108-0116
[16] Nader M N, Astaneh-Asl A. Shaking table test of rigid, semi-rigid and flexible steel frames. Journal of Structural Engineering 1996; ASCE; 122(6):589-96.
[17] Pirmoz A, Gholizadeh S. Predicting of moment-rotation behavior of bolted connections using neural networks, 2007, 3rd National Congress on Civil Engineering, University of Tabriz (3ncce).
[18] Pirmoz A, Performance of bolted angle connections in Progressive collapse of steel frames. Structural Design of Special and Tall Buildings, article in press. 2009.
[19] Pirmoz A. Evaluation of nonlinear behavior of bolted connections under dynamic loads. M.Sc. thesis, Tehran (Iran): K.N.Toosi University; 2006.
[20] Pirmoz A., Danesh F. The Seat Angle Role on Moment-Rotation Response of Bolted Angle Connections, Electronic Journal of Structural Engineering, 2009; Volume 9
[21] Pirmoz A, Danesh F, Farajkhah V. The effect of axial beam force on moment-rotation curve of top and seat angels connections, Structural Design of Special and Tall Buildings, article in press. 2009.
[22] Pirmoz A., Mohammadrezapour E., Seyed Khoei A., Saedi Daryan A. Moment-rotation behavior of bolted top-seat angle Journal of Constructional Steel Research, Volume 65, Issue 4, April 2009, Pages 973-984
[23] Pirmoz A., Saedi Daryan A., Mazaheri A., Ebrahim Darbandi H. Behavior of bolted angle connections subjected to combined shear force and moment, Journal of Constructional Steel Research 2008; 64: 436-46.
[24] Salajegheh E., Gholizadeh S, Pirmoz A. Self-organizing parallel back propagation neural networks for predicting the moment-rotation behavior of bolted connections, Asian Journal of Civil Engineering, 2008; 9 (6): 625-640.
[25] Shen J, Astaneh-Asl A. Hysteretic model of bolted-angle connections, Journal of constructional steel research 2000; 54: 317-343.
[26] Shen J., Astaneh-Asl A. Hysteretic behavior of bolted-angle connections. Journal of constructional steel research 1999; 51:201-18